



Luminescence properties of silver zinc phosphate glasses following different irradiations

C. Maurel^a, T. Cardinal^{a,*}, M. Bellec^b, L. Canioni^b, B. Bousquet^b, M. Treguer^a, J.J. Videau^a, J. Choi^{a,b,c}, M. Richardson^c

^a Institut de Chimie de la Matière Condensée de Bordeaux, CNRS UPR9048, Université de Bordeaux, 87 av. Dr. Schweitzer, 33608 Pessac Cedex, France

^b Centre de Physique Moléculaire Optique et Hertzienne, Université de Bordeaux, 351 Cours de la Libération, 33405 Talence Cedex, France

^c CREOL, The College of Optics & Photonics, University of Central Florida, Orlando, FL 32816-2700, USA

ARTICLE INFO

Available online 5 April 2009

Keywords:

Luminescence

Silver

Glass

Femtosecond laser irradiation

Clusters

ABSTRACT

We report on exposing a photosensitive zinc phosphate glass containing silver to different radiation (electron, gamma, optical). Laser irradiations using nanosecond ultraviolet (UV) and femtosecond infrared (IR) laser are compared with gamma and electron exposure. All irradiated glasses exhibit absorption maxima around 320 nm and 380 nm and emission in the visible spectral range. Following exposure, silver clusters are formed. The optical response of such species is investigated using absorption and fluorescence spectroscopic techniques. The mechanism of formation of these clusters is discussed.

© 2009 Elsevier B.V. All rights reserved.

1. Introduction

Recent interest has grown in the ability to change the optical characteristics, most notably the refractive index, of various silicate and phosphate glasses doped with silver by irradiation. Many diverse applications, waveguides [1–4], gratings [5–7], data-storage media [8], 3-D microstructures [9–11] and sensors, are possible with the controlled creation of precious metal (silver, gold, or copper) nanoparticles inside various glasses. There have been numerous techniques for Ag⁺-doped glass fabrication including sol–gel [12], ion-exchange [13], ion implantation [14] and melting/annealing [15]. Silver clusters or metallic nanoparticles can be synthesized by different irradiation methods: electron-beam [16], γ -ray [17,18], ultraviolet (UV) [19–21] or by femtosecond infrared (IR) laser [22–25]. A simplified description of the processes taking place at the level of the material can be presented. There exists a mobility threshold of the charge carriers corresponding, energetically, to a fundamental absorption band. One can then locally define, similar to a crystal, a forbidden band [26]. Thus, after the irradiation, the electrons pass from the valence band to the conduction band of the glass. Following this photoionization, the electrons are trapped by Ag⁺ ions forming neutral atoms of Ag⁰. In most cases identification of the induced silver species is not easy. It has been proposed, based on gamma-irradiated samples, that the trapping of the free electrons forms Ag⁰ and other more energetically favorable species (Ag₂⁺, Ag₃⁺) [18]. These species have specific spectral properties. Nevertheless,

in most cases these Ag_m^{x+} centers have not been clearly identified. In this work, we report a spectral study of the silver species created after different irradiation including femtosecond IR irradiation and leading to different optical signature. Comparison using different irradiation methods is presented.

2. Experimental

Samples of a phosphate glass 40P₂O₅–4Ag₂O–55ZnO–1Ga₂O₃ glass (mol%) were used to study the processes occurring after irradiation. Glasses were elaborated using standard melt-quench technique. Gallium oxide has been introduced to increase the glass stability. (NH₄)₂HPO₄, ZnO, AgNO₃ and Ga₂O₃ were used as raw materials and placed with appropriate amount in platinum crucible. A heating rate of about 1 °C min⁻¹ have been conducted up to 1000 °C and kept at this last temperature 1000 °C for 24–48 h. The liquid was then poured on bras mold after a short increase of the temperature at 1100 °C to access the appropriate viscosity. The obtained glass samples were annealed at 320 °C (55 °C below the glass transition temperature) for 3 h, cut (0.5–1 mm thick) and optically polished.

Absorption spectra were recorded using a double-beam spectrophotometer (CARY 5000 UV–VIS–NIR) between 200 and 800 nm.

Gamma irradiations were performed using ¹³⁷Cs source delivering 1.8 kGy h⁻¹. Irradiation with electron have been performed using electrons accelerator delivering train of 15 μ s pulses through a scanning beam (1–10 Hz) at a mean dose rate of 7 MGy h⁻¹.

UV laser irradiations were performed using a continuum Q-switched tripled Nd:YAG laser emitting at 355 nm with

* Corresponding author.

E-mail address: cardinal@icmcb-bordeaux.cnrs.fr (T. Cardinal).

repetition rate of 10 Hz and pulse energy of about 100 mJ. Millimeter size beam have been used for sample exposure.

For gamma electron and UV laser exposure on millimeter size sample area, emission and excitation spectra were collected using an Edinburgh Instruments FL 900 CDT spectrofluorometer equipped with a M30 monochromator connected to a photomultiplier tube (R955 Hamamatsu PMT) detector. A Xenon lamp (450 W) was used as the excitation source.

Femtosecond laser irradiations were performed using an Amplitude Systems TPulse 500 (Yb:KGW) 1030 nm source emitting 400 fs pulses at 10 MHz repetition rate. The laser mode is TEM₀₀ and the output polarization is TM. The maximum output power is 6 W which results in an energy per pulse maximum of 600 nJ.

The femtosecond laser was focused using a reflective 36 × objective with a 0.52 numerical aperture (working distance 15 mm) to a depth of 200 μm below the glass surface. The beam waist was estimated to be 1 μm. The glass was exposed to different irradiance levels between 5×10^{12} and 10×10^{12} W cm⁻² and different number of pulses from 100 to 10⁶. The sample was manipulated through patterning of bits with a bit spacing of 20 μm using a precision xyz stage. Epi-white light and epi-fluorescence microscopy were performed with commercial microscopes. A transmission confocal setup, with a 36 × 0.52 NA reflective objective, associated with Mercury (High-Pressure Nikon Hg HB-10101AF) and Xenon (Spectra-Physics Xe(Hg) 66906) lamps, was used for the emission and absorption spectroscopy. All spectra were measured using a spectrometer equipped with a CCD camera.

3. Results

3.1. Silver intrinsic luminescence in zinc phosphate glass

The glass exhibits an absorption cut-off (Fig. 1) at around 280 nm mainly due to the silver ions associated absorption. Fluorescence spectroscopy have been measured to investigate the emission of silver ions corresponding to dipolar electric transition $4d^{10} \rightarrow 4d^9 5s^1$. The main feature is composed of an excitation band at 265 nm and a corresponding emission at 380 nm. Such emission has been previously attributed to isolated Ag⁺ silver ions. Weaker excitation band can be recorded for excitation at around

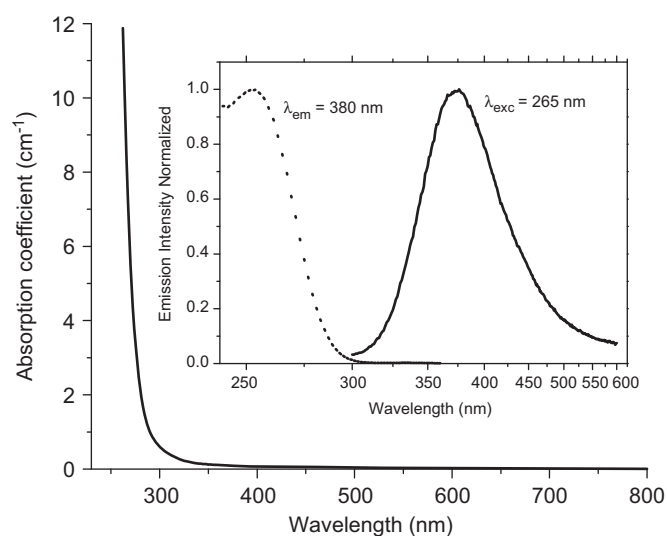


Fig. 1. Absorption spectrum of the glass sample, inset: emission spectrum for excitation at 265 nm and excitation spectrum for emission at 380 nm.

360 nm leading to emission between 500 and 800 nm. This last intrinsic fluorescence is due to Ag⁺–Ag⁺ pairs. Lifetimes of excited levels corresponding to both emissions are, respectively 25 μs and 125 μs at room temperature [15].

3.2. Gamma and electron exposure

Continuous gamma irradiations have been conducted for different exposure times on 1-mm-thick samples. The corresponding absorption spectra are reported in Fig. 2a. Two absorption bands appear at around 325 and 380 nm after gamma exposure. The relative intensity evolution of these bands seems to be identical for the doses used. The appearance of these absorption features are related to the decrease of the emission intensity at 380 nm for excitation at 260 nm attributed to isolated silver ions. The evolution of the area integrated under this last emission can be plotted against the dose or the exposure time as shown in Fig. 2a (inset). The decrease of the integrated intensity can be fitted with a first-order kinetic equation. This evolution is in accordance with a progressive disappearing of silver ions after irradiation.

Emission spectra are reported in Fig. 2b for excitation in the gamma-induced absorption band. Excitation around 320 nm leads to a broad emission band from 450 up to 800 nm with a band located around 500 nm and second band around 620 nm. On the excitation spectra for emission at 630 nm two bands at 320 and 380 nm can be observed for the two lowest doses. The highest dose gives rise to a new shoulder at 290 nm. Excitation between 360 and 400 nm give rise to a intense emission component centered at around 500 nm as compared to the 620 nm one. One has to mention that for the largest dose, the relative intensity of the band at 500 nm increases, indicating that different natures of luminescent centers are most likely occurring.

In the case of electron, the electron accelerator allows, using a high dose rate, the formation of high density of electron traps. The results are compared to gamma exposure for long time exposure as shown in Fig. 2c. Emission spectra, compared for excitation at 380 nm reveal a significant increase of the emission at 500 nm for sample irradiated with the largest gamma dose and for exposure to the electron beam. The existence of this emission band can be related to the formation of significant amount of Ag⁰ center within the glass network.

3.3. UV laser irradiation

A fluence of 640 mJ/cm² per pulse has been used for the UV laser irradiation. Linear absorption features recorded in the irradiated area, not shown, are similar to the spectra reported in Fig. 2a with absorption band, respectively, at 320 and 380 nm increasing in intensity with the number of pulses. Even if quantitative measurement is difficult, much lower absorption features are observed as compared to gamma and electron exposures. Single emission at 620 nm is observed even for exposure with 600 pulses for different excitation at 320, 365 and 380 nm (Fig. 3b). No feature can be observed at around 290 nm in the excitation spectrum (Fig. 3a). Similarly with gamma and electron exposure, the emission at 380 nm for excitation at 260 nm attributed to isolated silver ions decrease in intensity in the UV laser-irradiated zone.

3.4. Femtosecond laser exposure

Fig. 4a shows the difference in absorbance between the IR femtosecond laser-irradiated and non-irradiated regions. Micro-meter size laser spot has been used for writing. Absorption spectra

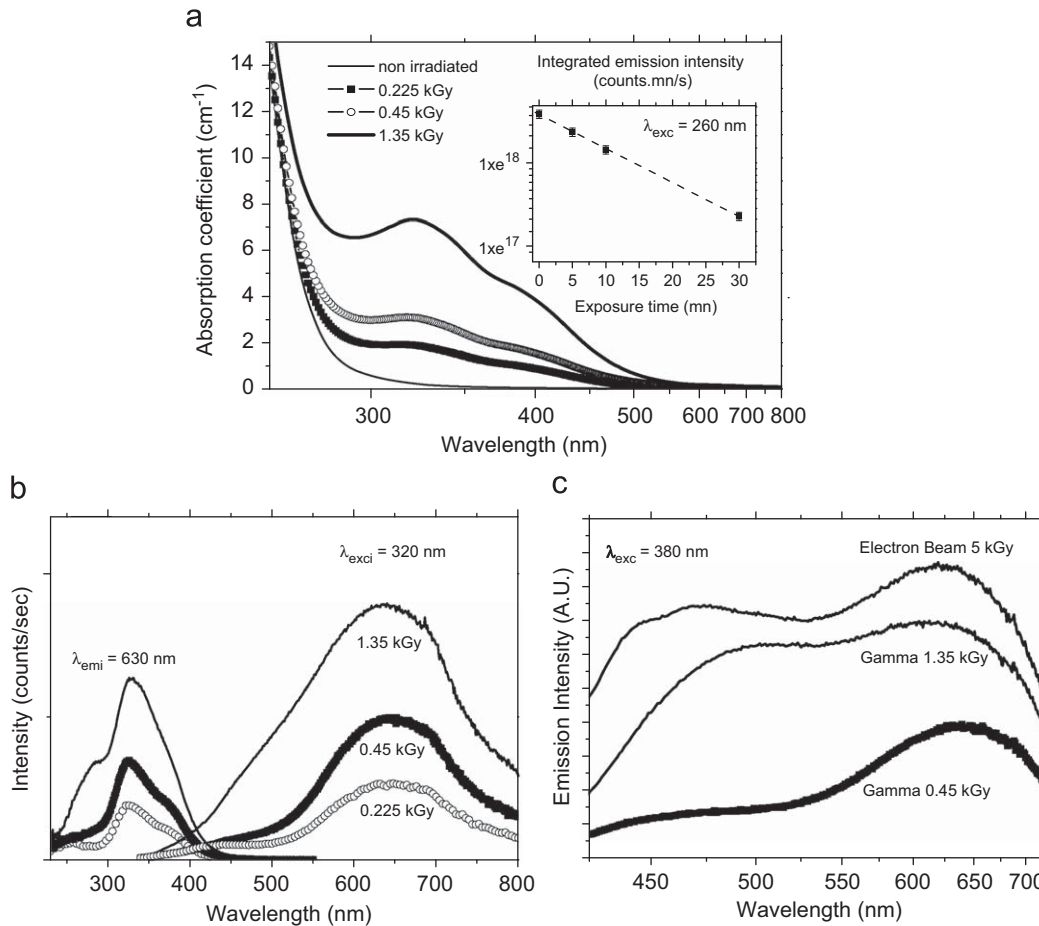


Fig. 2. (a) Absorption spectra corresponding to different gamma irradiation doses 5 min (0.225 kGy), 10 min (0.45 kGy), 30 min (1.35 kGy) and resulting luminescence properties: (b) excitation spectra for emission at 630 nm and emission spectra for excitation at 320 nm and (c) for excitation at 380 nm.

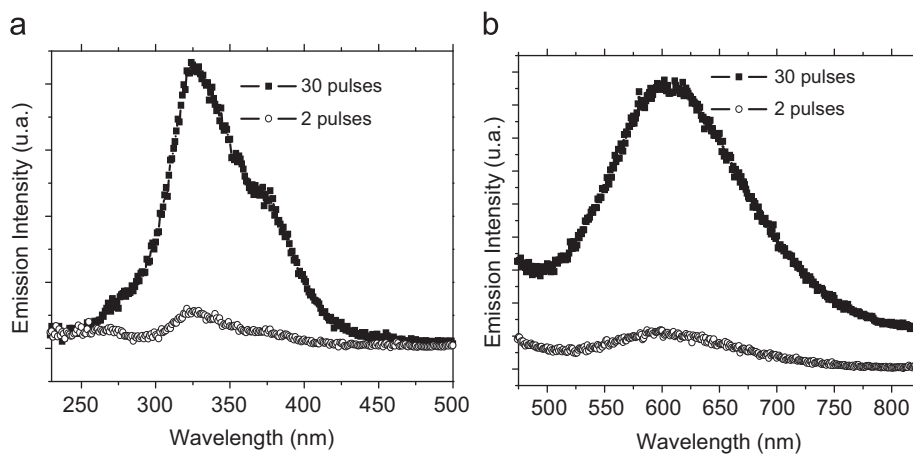


Fig. 3. (a) Excitation spectra for emission at 620 nm and (b) emission spectra for excitation at 320 nm following two different irradiation doses with nanosecond UV laser emitting at 355 nm.

were collected between 250 and 350 nm to obtain an intense enough signal. An absorption band from 280 up to 340 nm can be observed. The decrease of the absorption above 340 nm is due to absorption filter used for recording. Emission spectrum, registered for excitation at 365 nm, exhibit a main contribution at around 500 nm and a second one at around 600 nm (Fig. 4b).

Transmission and fluorescence microscopy images of spots irradiated with different irradiance level (x -axis) and number of

pulses (y -axis) are shown in Fig. 4c. Above $8 \times 10^{12} \text{ W cm}^{-2}$, clear damage could be distinguished. Below this threshold, weak linear index changes are visible and fluorescence of silver species is observed. With increasing the number of pulses (up 10^6), the fluorescence grows up and saturates proving again the consumption of silver ions. It has to be noticed that the fluorescence is occurring in a cylindrical shell localized on the edge of the irradiated zone. No fluorescence could be detected in the center of the exposed area.

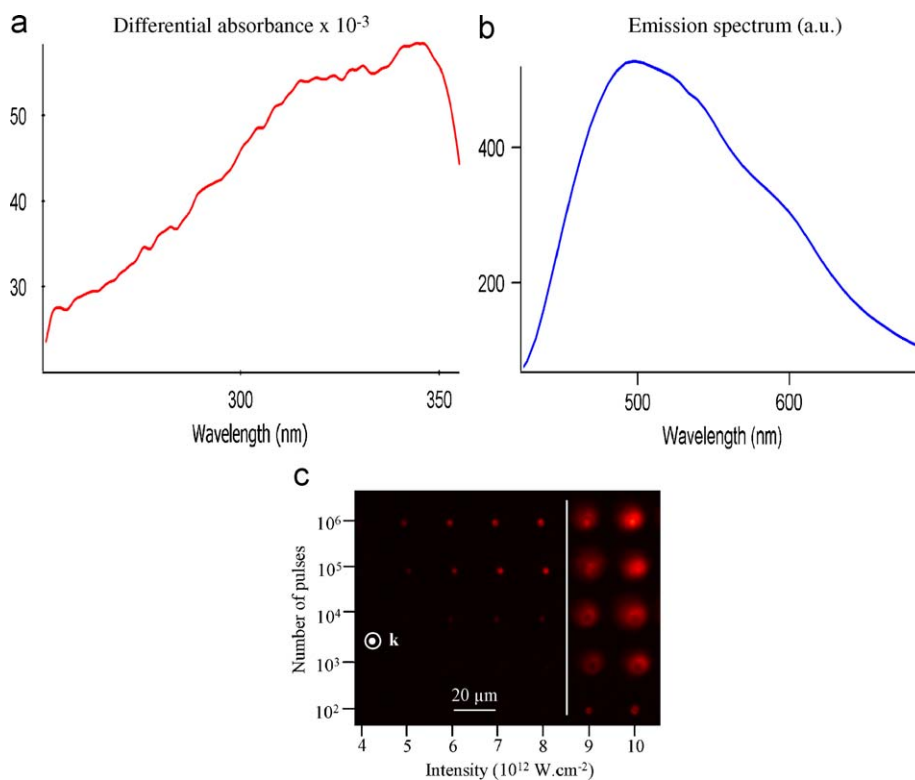
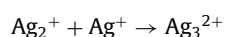
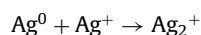
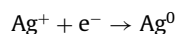


Fig. 4. (a) Absorption and (b) emission spectra of the irradiated region using femtosecond laser emitting at 1030 nm ($I = 6.10^{12} \text{ W cm}^{-2}$, $N = 10^6$) recorded for excitation at 365 nm. (c) Fluorescence microscopy images for excitation at 365 nm after IR femtosecond laser irradiation for different intensity and fluence.

4. Discussion

Even if the mechanisms of formation of hole and electron traps are different, in all the irradiation cases, the 500 and 620 nm peak observed in the emission spectrum is believed to be due to aggregation of Ag^0 and Ag^+ ions which have possibly generated additional chemically stable clusters Ag_m^{x+} such as Ag_2^+ , Ag_3^{2+} , ... [18,27]. These species have specific absorption and emission features as it has been demonstrated for instance in liquid phase [28,29]. Up to now, still, no clear assignments have been proposed to clearly attribute the emission bands located at 620 and 500 nm in glasses. Nevertheless, comparison using different irradiation sources can be drawn. Syutkin et al. have proposed by combining optical data and EPR study for gamma-irradiated silver phosphate glasses that emission around 620 nm for excitation around 320 nm is due to a oxidized silver cluster Ag_3^{2+} . The process of formation of such species can be described as follows:



Following irradiation, electron and hole traps are produced. The electron traps Ag^0 combined with Ag^+ ions to form Ag_2^+ species and later Ag_3^{2+} emitting centers. Influence of gamma radiation dose have shown modification of the relative intensity of the 500 and 620 nm emission components indicating most probably the presence of different clusters Ag_m^{x+} with different m/x ratio. Electron irradiation is confirming this evolution with a strong emission component at around 500 nm. All these observations are consistent with a decrease of the emission of isolated silver ions showing that silver is definitely acting as the electron trap. UV

irradiation at 355 nm close to the band edge of the glass clearly corresponds to lower formation of electron traps. Lower intensity of the absorption bands around 320 nm has been measured. Single emission band at around 620 nm could be observed for excitation at 320 nm. Femtosecond laser irradiation leads to emission at around 530 and 620 nm which is very similar to gamma and electron irradiation but mainly in a cylindrical shell localized on the edge of the irradiated zone. In this case, multiphoton absorption phenomenon of photon at 1030 nm is proposed to be at the origin to the absorption corresponding to valence band to conduction band transition. Localization of the emission at the surrounding of the irradiated area has been assigned to heat accumulation due to the high repetition rate of the laser and migration of silver ions and atoms. Full understanding of the phenomenon is under investigation. According to the other irradiations methods, such emission around 530 nm should result from a local high quantity of silver electron trap centers Ag^0 and a large amount of induced free carriers. We can propose that in this latter case, silver cluster Ag_m^{x+} with a high ratio m/x are formed even though the formation of Ag_3^{2+} is occurring. It is not clear if the Ag_3^{2+} species can be considered as the seed of the center emitting at 500 nm.

In parallel to the electron traps, Ag^{2+} hole centers formation have been proposed in different study [19,30,31]. In our case, no specific absorption features associated to such species have been identified, complete EPR study is necessary. Nevertheless, oxydo-reduction processes involving two silver ions or one silver ion and a phosphate group leading to the formation of hole centers Ag^{2+} or PO_4^{2-} and Ag^0 can be proposed, as previously suggested for instance for gamma-irradiated samples [18]. As Ag^0 center is not stable, interaction with the silver ions Ag^+ is taking place to form Ag_m^{x+} silver clusters. Dependency with the mobility of silver ions should be an important issue in the formation of silver clusters [18], in particular when local heating is occurring.

The local stabilization of these Ag_m^{x+} emitting species in the IR femtosecond laser-irradiated area (focal volume) proves the nonlinear interaction regime.

5. Conclusion

Femtosecond IR pulses irradiation leads to the localized formation of Ag_m^{x+} silver clusters mixing of Ag^0 and Ag^+ , which are more stable than neutral atom Ag^0 . Comparisons with different irradiation method have been studied and influence of the amount of silver Ag^0 electron traps on the optical response is proposed. A mechanism of formation of silver clusters has been proposed. Fluorescent structures inside the glass have been observed in the focal volume optical voxel.

Acknowledgements

This work was carried out with the support of a number of research, equipment and educational French and US grants, including the Agence Nationale de la recherche ANR (Grant ANR-05-BLAN-0212-01), the CNRS PICS Grant 3179, a FACE grant from the French Embassy in the US, and an international REU NSF Grants (EEC-0244109 and DMR-031208).

References

- [1] K.M. Davis, K. Miura, N. Sugimoto, K. Hirao, *Opt. Lett.* 21 (1996) 1729.
- [2] K. Miura, Jianrong Qiu, H. Inouye, T. Mitsuyu, K. Hirao, *Appl. Phys. Lett.* 71 (1997) 23.
- [3] J. Chan, T. Huser, S. Risbud, J. Hayden, D. Krol, *Appl. Phys. Lett.* 82 (2003) 2371.
- [4] H. Ebendorff-Heidepriem, *Opt. Mater.* 25 (2004) 109.
- [5] Y. Li, W. Watanabe, K. Yamada, T. Shinagawa, K. Itoh, J. Nishii, Y. Jiang, *Appl. Phys. Lett.* 80 (2002) 1508.
- [6] Oleg M. Efimov, Leonid B. Glebov, Larissa N. Glebova, Kathleen C. Richardson, Vadim I. Smirnov, *Appl. Opt.* 38 (1999) 619.
- [7] Y. Cheng, K. Sugioga, M. Masuda, K. Shihoyama, K. Toyoda, K. Midorikawa, *Opt. Express* 11 (2003) 15.
- [8] H. Ditzbacher, J.R. Krenn, B. Lamprecht, A. Leitner, F.R. Aussenegg, *Opt. Lett.* 25 (2000) 563.
- [9] M. Masuda, K. Sugioka, Y. Cheng, N. Aoki, M. Kawachi, K. Shihoyama, K. Toyoda, H. Helvajian, K. Midorikawa, *Appl. Phys. A* 76 (2003) 857.
- [10] Y. Cheng, K. Sugioka, K. Midorikawa, M. Masuda, K. Toyoda, M. Kawachi, K. Shihoyama, *Opt. Lett.* 28 (2003) 1144.
- [11] M. Masuda, K. Sugioka, Y. Cheng, N. Aoki, M. Kawachi, K. Shihoyama, K. Toyoda, K. Midorikawa, *SPIE Proc.* 4830 (2002) 576.
- [12] M.A. García, S.E. Paje, J. Llopis, M.A. Villegas, J.M. Fernández Navarro, *J. Phys. D* 32 (1999) 975.
- [13] G. De Marchi, F. Caccavale, F. Gonella, G. Mattei, P. Mazzoldi, G. Battaglin, A. Quaranta, *Appl. Phys. A* 63 (1996) 403.
- [14] A. Stepanov, V. Popok, *Surf. Coat. Technol.* 185 (2004) 30.
- [15] I. Belharouak, C. Parent, B. Tanguy, G. Le Flem, M. Couzi, *J. Non-Cryst. Solids* 244 (1999) 238.
- [16] H. Hofmeister, S. Thiel, M. Dubiel, E. Schurig, *Appl. Phys. Lett.* 70 (1997) 13.
- [17] A. Pan, H. Zeng, Z. Yang, F. Liu, Z. Ding, Y. Qian, *Mater. Res. B* 38 (2003) 789.
- [18] A. Dmitryuk, S. Parmzina, A. Perminov, N. Solov'eva, N. Timofeev, *J. Non-Cryst. Solids* 202 (1996) 173.
- [19] S. Stookey, *Ind. Eng. Chem.* 41 (1949) 856.
- [20] Y. Watanabe, G. Namikawa, T. Onuki, K. Nishio, T. Tsuchiya, *Appl. Phys. Lett.* 78 (2001) 2125.
- [21] L. Glebov, *Opt. Mater.* 25 (2004) 413.
- [22] J. Qiu, M. Shirai, T. Makaya, J. Si, X. Jiang, C. Zhu, K. Hirao, *Appl. Phys. Lett.* 81 (2002) 3040.
- [23] N. Takeshima, Y. Kuroiwa, Y. Narita, S. Tanaka, K. Hirao, *J. Non-Cryst. Solids* 336 (2004) 234.
- [24] Q. Zhao, J. Qiu, X. Jiang, C. Zhao, C. Zhu, *Opt. Express* 12 (2004) 4035.
- [25] H. Zeng, J. Qiu, X. Jiang, C. Zhu, F. Gan, *J. Phys. Condens. Matter* 16 (2004) 2901.
- [26] O.M. Efimov, L.B. Glebov, S. Grantham, M. Richardson, *J. Non-Cryst. Solids* 253 (1999) 58.
- [27] A. Podlipensky, V. Grebenev, G. Seifert, H. Graener, *J. Lumin.* 109 (2004) 135.
- [28] A. Henglein, *J. Phys. Chem.* 97 (1993) 5457.
- [29] M. Tréguer, F. Rocco, A. Le Nestour, T. Cardinal, *Solid State Sci.* 7 (2005) 812.
- [30] V.M. Syutkin, V.A. Tolkathev, A.V. Dmitryuk, S.E. Paramzina, *Chem. Phys.* 196 (1995) 139.
- [31] Y. Watanabe, G. Namikawa, T. Onuki, K. Nishio, T. Tsuchiya, *Appl. Phys. Lett.* 78 (15) (2001) 2125.